Phys. Lett. B 849 (2024) 138454

Contents lists available at ScienceDirect

Physics Letters B

journal homepage: www.elsevier.com/locate/physletb

Letter

2^{++} Tensor di-gluonium from Laplace sum rules at NLO

Siyuan Li [a], Stephan Narison [b], Tom Steele [a], Davidson Rabetiarivony [c]

[a] Department of Physics & Engineering Physics, University of Saskatchewan, SK, S7N 5E2, Canada
[b] Laboratoire Univers et Particules de Montpellier, CNRS-IN2P3, Case 070, Place Eugène Bataillon, 34095, Montpellier, France
[c] Insitute of High-Energy Physics (iHEPMAD), Univ. Ankatso, Antananarivo, Madagascar

ARTICLE INFO

Editor: A. Ringwald

Keywords:
QCD spectral sum rules
Meson decay constants
Light quark masses
Chiral symmetry

ABSTRACT

We evaluate the next-to-leading (NLO) corrections to the perturbative (PT) and $\langle\alpha_s G^2\rangle$ condensate and the LO constant term of the $\langle G^3\rangle$ contributions to the 2^{++} tensor di-gluonium two-point correlator. Using these results into the inverse Laplace transform sum rules (LSR) moments and their ratio, we estimate the mass and coupling of the lowest ground state. We obtain: $M_T = 3028(429)$ MeV and the renormalization group invariant (RGI) coupling $\hat{f}_T = 167(40)$ MeV within a vacuum saturation estimate of the $D = 8$ dimension gluon condensates ($k_G = 1$). We study the effect of k_G on the result and find: $M_T = 3188(405)$ MeV and $\hat{f}_T = 164(28)$ MeV for $k_G = (3 \pm 2)$. Absolute upper bounds for the mass and coupling from the positivity of the spectral function are also derived. Our result does not favour the pure gluonia/glueball nature of the observed $f_2(2010, 2300, 2340)$ states.

1. Introduction

Since the pioneering work of Novikov et al. (NSVZ) [1], some efforts have been done for improving the determination of the 2^{++} tensor di-gluonium mass and coupling either using a least-square fit method [2] or stability criteria [3,4]).[1] To Lowest Order (LO) of perturbative QCD (PT) and including the dimension $d = 8$ condensates estimated by (SVZ) [6] using vacuum saturation, the up-to-date results are [4][2]:

$$f_T|_{LO} = 113(20)\ \text{MeV},$$
$$M_T|_{LO} = 2.0(1)\ \text{GeV}, \quad M_T|_{LO} \leq 2.7(4)\ \text{GeV}. \tag{1}$$

In this paper, we shall improve these LO results by including NLO corrections and checking the effect of the violation of vacuum saturation on the results.

2. The QCD 2^{++} di-gluonium two-point function

We shall be concerned with the two-point function[3]:

$$\psi_T^{\mu\nu\rho\sigma}(q^2) \equiv i\int d^4x\, e^{iqx}\langle 0|\theta_G^{\mu\nu}(x)\left(\theta_G^{\rho\sigma}\right)^\dagger(0)|0\rangle$$
$$= \left(P^{\mu\nu\rho\sigma} \equiv \eta^{\mu\rho}\eta^{\nu\sigma} + \eta^{\mu\sigma}\eta^{\nu\rho} - \frac{2}{n-1}\eta^{\mu\nu}\eta^{\rho\sigma}\right)\psi_T(q^2), \tag{2}$$

built from the gluon component of the energy-momentum tensor[4]:

$$\theta_G^{\mu\nu} = \alpha_s\left[-G_\alpha^{\mu,a}G_a^{\nu\alpha} + \frac{1}{4}g^{\mu\nu}G_{\alpha\beta}^a G_a^{\alpha\beta}\right], \tag{3}$$

with:

$$\eta^{\mu\nu} \equiv g^{\mu\nu} - q^\mu q^\nu/q^2 \ : \quad P_{\mu\nu\rho\sigma}P^{\mu\nu\rho\sigma} = 2(n^2 - n - 2)\,, \tag{4}$$

where: $n = 4 + 2\epsilon$ is the space-time dimension used for dimensional regularization and renormalization. To LO and up to dimension $D = 8$ gluon condensates, the QCD expression is [1]:

$$\psi_T|_{LO}(q^2 \equiv -Q^2) = a_s^2\left[-\frac{Q^4}{20}\log\frac{Q^2}{\nu^2} + \frac{5}{3}\pi^3\alpha_s\langle 2O_1 - O_2\rangle\right], \tag{5}$$

where $a_s \equiv \alpha_s/\pi$ and:

$$O_1 = \left(f_{abc}G_{\mu\alpha}G_{\nu\alpha}\right)^2, \quad O_2 = \left(f_{abc}G_{\mu\nu}G_{\alpha\beta}\right)^2. \tag{6}$$

Using the vacuum saturation hypothesis ($k_G = 1$), it reads [1]:

E-mail addresses: siyuan.li@usask.ca (S. Li), snarison@yahoo.fr (S. Narison), tom.steele@usask.ca (T. Steele), rd.bidds@gmail.com (D. Rabetiarivony).

[1] For recent reviews on the status of gluonia/glueballs, see e.g. [5] and references quoted therein.

[2] Tachyonic gluon mass contribution though important for recovering the universal scale of the gluonia channels does not contribute in the unsubtracted sum rule analysis as it has no imaginary part [7]. We have rescaled the normalization of the coupling by a factor $\sqrt{2}$.

[3] For relations among different form factors, see e.g. [7].

[4] Notice the extra-factor α_s compared to the current used in Ref. [4] and references quoted therein.

https://doi.org/10.1016/j.physletb.2024.138454
Received 4 September 2023; Received in revised form 19 December 2023; Accepted 9 January 2024
Available online 17 January 2024

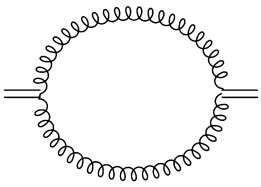

Fig. 1. LO perturbative contribution to $\psi_T(Q^2)$.

$$\langle 2O_1 - O_2\rangle \simeq -k_G\left(\frac{3}{16}\right)\langle G^2\rangle^2. \tag{7}$$

We shall test the effect of this assumption by taking:

$$k_G \neq 1, \tag{8}$$

for an eventual violation of the factorization assumption like the one found for the $D=6$ four-quark condensates (see e.g. [3,8–10]) where this assumption is violated by about a factor 5-6.

3. PT expression of the two-point function up to NLO

• *Lowest Order (LO) contribution*

It comes from the diagram in Fig. 1 and reads:

$$\psi_T^{pert}|_{LO} = -a_s^2\frac{Q^4}{20}\log\frac{Q^2}{\nu^2} \tag{9}$$

• *Next-to-Leading (NLO) contribution*

We use two approaches to perform the calculation:

◇ *Diagrammatic renormalization*

This approach has been initiated in [11] for QCD sum-rule correlation functions. It requires an isolation of the subdivergences arising from the one-loop subdiagram(s) of an individual bare NLO diagram (see e.g., Ref. [12]). Counterterm diagrams generated from the subdivergences are then calculated and subtracted from the bare diagram to obtain the renormalized diagram. A self-consistency check of the method is the cancellation of non-local divergences in each diagram.

We shall be concerned with the bare diagrams a–g listed in Table 1 and their corresponding individual diagrammatically-renormalized contributions parametrized in Feynman gauge as:

$$\psi_T^{pert}|^{diag}_{NLO}(Q^2) = a_s^3\left(\frac{Q^4}{16}\right)\log\frac{Q^2}{\nu^2}\left[A\log\frac{Q^2}{\nu^2} + B\right] \tag{10}$$

with: $a_s \equiv \alpha_s/\pi$. The sum of the contributions of the bare diagrammatically-renormalized diagrams a–g in Table 1 leads to the renormalized NLO two-point function for n_f flavours:

$$\psi_T^{pert}|^{R}_{NLO}(Q^2) = a_s^3\left(\frac{Q^4}{16}\right)L\left[-\frac{2}{15}n_f L + \left(\frac{4}{3} + \frac{202}{225}n_f\right)\right], \tag{11}$$

with: $L = \log\frac{Q^2}{\nu^2}$. Note that diagram h from Table 1 is not used in the diagrammatic renormalization method, but is crucial in the conventional renormalization approach for the cancellation of the non-local $(1/\epsilon)\log(Q^2/\nu^2)$ as we shall see in the next section.

◇ *The conventional approach*

Here, we calculate each QCD diagram using the standard Feynman approach (see e.g. [3,8,13]). We consider the renormalization of the gluonic current using the renormalization constant obtained in Ref. [14] for the current $\theta_G^{\mu\nu}/\alpha_s$:

$$Z_\psi = 1 - \left(\frac{n_f}{3}\right)\frac{a_s}{2\epsilon} \tag{12}$$

for $n = 4 + 2\epsilon$ dimensions to which corresponds the anomalous dimension:

$$\gamma_\psi \equiv \left(\gamma_1 = \frac{n_f}{3}\right)a_s. + \cdots. \tag{13}$$

Taking into account the renormalization of α_s:

$$Z_{\alpha_s} = 1 + \beta(\alpha_s)\frac{1}{2\epsilon}, \tag{14}$$

one can deduce the anomalous dimension of the current $\theta_G^{\mu\nu}$:

$$\gamma_\psi^\theta \equiv \left(\gamma_1^\theta = -\frac{11}{2}\right)a_s. + \cdots. \tag{15}$$

The diagrams appearing in Table 1e) to g) are due to the non-abelian property of QCD where:

$$G_{\mu\nu}^{(a)} = \partial_\mu A_\nu^{(a)} - \partial_\nu A_\mu^{(a)} + g f^{abc} A_\mu^{(b)} A_\nu^{(c)} \tag{16}$$

The diagram in Table 1h) is induced by the off-diagonal term which arises due to the mixing of the $\bar{q}q$ and G^2 currents. Following [14,15], such terms are necessary to cancel the non-local $(1/\epsilon)$ log (Q^2/ν^2) divergent terms appearing in the calculations given in Table 1. It is remarkable to notice that there is a systematic factor two difference for the coefficient A of diagrams a) to g) from the two approaches. The sum of the individual diagrams in Table 1 gives for the current normalized in Eq. (3):

$$\psi_T^{RI}|_{NLO}(Q^2) = \frac{a_s^3}{600}Q^4\log\frac{Q^2}{\nu^2}\,n_f\left[5\left(\log\frac{Q^2}{\nu^2} + \frac{2}{\epsilon}\right) - 9\right] \tag{17}$$

◇ *NLO PT results*

We have shown in the previous sections, that the diagrammatic and conventional approaches lead to the same result. The renormalized two-point function for n_f flavours reads:

$$\psi_T^{pert}|^{R}_{NLO}(Q^2) \equiv \psi_T^{pert}|_{LO} + \psi_T^{pert}|^{B}_{NLO} + \psi_T^{RI}|_{NLO} =$$
$$\psi_T^{pert}|_{LO}\left[1 + a_s\left(\frac{n_f}{6}\log\frac{Q^2}{\nu^2} - \frac{101n_f + 150}{90}\right)\right], \tag{18}$$

where $\psi_T^{pert}|_{LO}$ can be deduced from Eq. (5). One can notice that for gluodynamics ($n_f = 0$), we recover the earlier result of [16].

4. Dimension-four gluon $\langle\alpha_s G^a_{\mu\nu}G^{\mu\nu}_a\rangle$ condensate

One can notice from Eq. (5) that, unlike the case of scalar and pseudoscalar gluonia [1], the contributions of the gluon condensates are only due to the $D=8$ dimension.

• *LO contribution*

From the diagram in Fig. 2, we have checked that to LO the leading log-term does not contribute to the two-point function. The LO contribution comes from the constant term:

$$\psi_T^{G^2}|_{LO} = \frac{\alpha_s}{6}\langle\alpha_s G^2\rangle, \tag{19}$$

where we have used two different approaches (plane wave and conventional one using the projection in Eq. (2)). The non-zero value of this constant term raises the question of the validity of the null result obtained in Ref. [17] based on instantons for dual/antidual background fields. However, this term is harmless in the LSR analysis as it will disappear when one takes the different derivatives of the two-point functions.

• *NLO contribution*

Table 1
NLO perturbative contribution to $\psi_T(Q^2)$ in conventional and diagrammatic renormalization methods. The quantities A and B are defined in Eq. (10). Diagrams h) are only used in conventional renormalization but are not applicable (N/A) in the diagrammatic method.

Label	NLO Diagrams	Conventional		Diagrammatic	
		A	B	A	B
a)	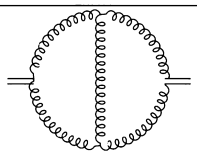	$-\frac{7}{30}$	$\frac{3017}{1800}-\frac{7}{30\epsilon}$	$-\frac{7}{60}$	$-\frac{1151}{1800}$
b)	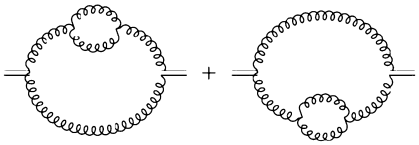	$\frac{19}{10}$	$-\frac{1321}{150}+\frac{19}{10\epsilon}$	$\frac{19}{20}$	$-\frac{2129}{300}$
c)	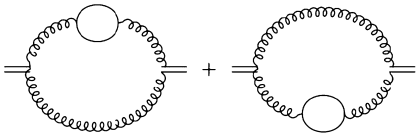	$-\frac{4}{15}n_f$	$\frac{256}{225}n_f-\frac{4}{15\epsilon}n_f$	$-\frac{2}{15}n_f$	$\frac{202}{225}n_f$
d)	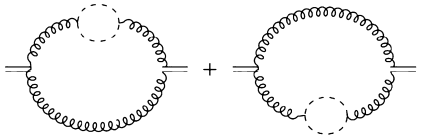	$\frac{1}{10}$	$-\frac{79}{150}+\frac{1}{10\epsilon}$	$\frac{1}{20}$	$-\frac{131}{300}$
e)	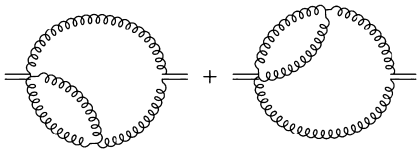 + Sym	$-\frac{31}{10}$	$\frac{2887}{200}-\frac{31}{10\epsilon}$	$-\frac{31}{20}$	$\frac{7637}{600}$
f)	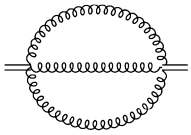	0	-1	0	-1
g)	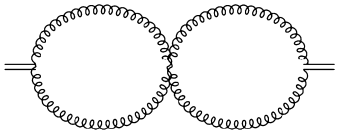	$\frac{4}{3}$	$-\frac{40}{9}+\frac{4}{3\epsilon}$	$\frac{2}{3}$	$-\frac{20}{9}$
h)	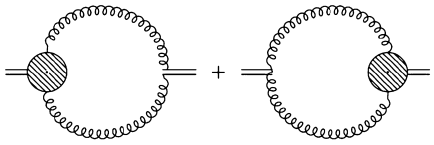	$\frac{2}{15}n_f$	$-\frac{6}{25}n_f+\frac{4}{15\epsilon}n_f$	N/A	N/A
Total		$-\frac{2}{15}n_f$	$\frac{202}{225}n_f+\frac{4}{3}$	$-\frac{2}{15}n_f$	$\frac{202}{225}n_f+\frac{4}{3}$

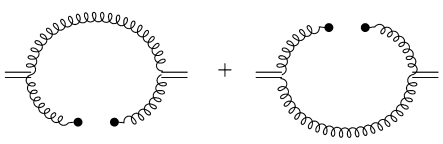

Fig. 2. LO $\alpha_s G^2$ contribution to $\psi_T(Q^2)$.

The leading-log. contribution at NLO, can be derived from the renormalization group equation (RGE). Using the fact that $\langle\alpha_s G^2\rangle$ obeys the RGE [18] (see different applications in section 4.4 of [13])[5]:

$$\left\{-\frac{\partial}{\partial t}+\beta(a_s)\,a_s\frac{\partial}{\partial a_s}-2\gamma_\psi^\theta\right\}\psi_T^{G^2}=0 \tag{20}$$

where $t\equiv(1/2)\log(Q^2/\nu^2)$ and γ_ψ^θ is the anomalous dimension defined in Eq. (15). Writing the α_s expansion as:

$$\psi_T^{G^2}=\left(g_0\alpha_s^2+2g_1\alpha_s^2a_s\,t+g_1'\alpha_s^2a_s-2\gamma_\psi^\theta\alpha_s^2+\cdots\right)\langle G^2\rangle, \tag{21}$$

and considering that $\langle\alpha_s G^2\rangle$ is a constant, one deduces:

$$g_1=g_0\left(\frac{\beta_1}{2}-\gamma_1^\theta\right)=\frac{1}{24}\left(11+\frac{2n_f}{3}\right)\quad\text{with:}\quad g_0=\frac{1}{6}. \tag{22}$$

Note that, e.g. diagrams e) and f) in Table 1 contribute to g_1' and will disappear after taking the 3rd derivative of the two-point correlator for extracting the LSR expression.

[5] We take into account the overall α_s factor appearing in the definition of the energy-momentum tensor current.

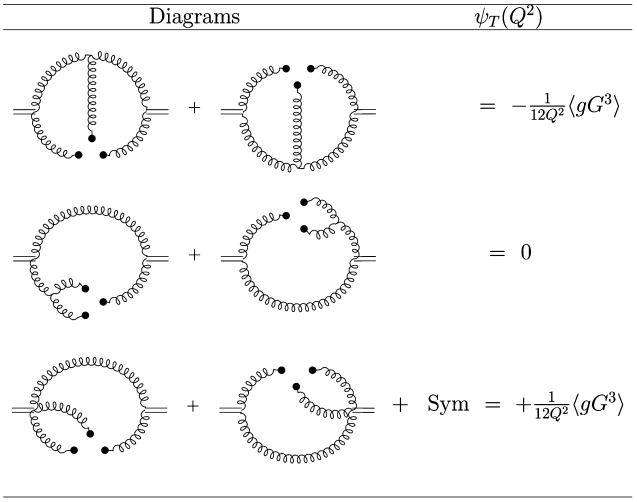

Fig. 3. LO $g\langle G^3\rangle$ contribution to $\psi_T(Q^2)/\alpha_s^2$.

5. Dimension-six $g^3\langle f_{abc}G^a_{\mu\nu}G^b_{\nu\rho}G^c_{\rho\mu}\rangle$ gluon condensate

• *LO contribution*

We calculate the coefficients of the $\langle gG^3\rangle$ contribution using the conventional approach and the projection in Eq. (4). We show the different contributions in Fig. 3 where the total sum is zero (log. coefficient and constant term) in agreement with the result of [17].

• *Check of the result*

We recompute the G^3 coefficient of the scalar gluonium two-point function using the same method. We recover the result of Ref. [1] which is an indirect test of our result.

6. Laplace Sum Rule (LSR) analysis

• *QCD expression*

Collecting the previous results, we obtain for $n_f = 3$ flavours to order α_s and up to dimension-8 condensates:

$$\tilde{\psi}_T(Q^2) \equiv \frac{\psi_T(Q^2)}{\alpha_s^2}$$
$$= -\frac{1}{20\pi^2}Q^4\log\frac{Q^2}{\nu^2}\left[1 + a_s\left(\frac{1}{2}\log\frac{Q^2}{\nu^2} - \frac{151}{30}\right)\right]$$
$$+\frac{13}{24\pi}\langle\alpha_s G^2\rangle\log\frac{Q^2}{\nu^2} - \frac{5\pi}{16}\frac{k_G\alpha_s\langle G^2\rangle^2}{Q^4}. \quad (23)$$

We shall be concerned with the following inverse Laplace transform moments and their ratio [6,19–22]:

$$\mathcal{L}^c_{0,1}(\tau,\mu) = \int_{t>}^{t_c} dt\, t^{(0,1)} e^{-t\tau}\frac{1}{\pi}\mathrm{Im}\tilde{\psi}_T(t,\nu)\,,$$
$$\mathcal{R}^c_{10}(\tau) \equiv \frac{\mathcal{L}^c_1}{\mathcal{L}^c_0} = \frac{\int_{t>}^{t_c} dt\, e^{-t\tau} t\,\mathrm{Im}\tilde{\psi}_T(t,\nu)}{\int_{t>}^{t_c} dt\, e^{-t\tau}\mathrm{Im}\tilde{\psi}_T(t,\nu)}, \quad (24)$$

To get the lowest moment $\mathcal{L}^c_0$, we take the 3rd derivative of the two-point function which is superconvergent while for the $\mathcal{L}^c_1$ moment, we take the 4th derivative of $Q^2\tilde{\psi}_T(Q^2)$. The NLO QCD expressions of the moments for $n_f = 3$ flavours are:

$$\mathcal{L}^c_0 = \frac{\tau^{-3}}{10\pi^2}\left\{\left[1 - a_s\left(\frac{53}{15} + \gamma_E\right)\right]\rho^c_2 - \frac{65\pi}{12}\langle\alpha_s G^2\rangle\tau^2\rho^c_0\right.$$
$$\left. -\frac{\pi^2}{a_s}\left(\frac{25}{8}\right)k_G\langle\alpha_s G^2\rangle^2\tau^4\right\}, \quad (25)$$

and

$$\mathcal{L}^c_1 = \frac{3\tau^{-4}}{10\pi^2}\left\{\left[1 - a_s\left(\frac{16}{5} + \gamma_E\right)\right]\rho^c_3 - \frac{65\pi}{36}\langle\alpha_s G^2\rangle\tau^2\rho^c_1\right.$$
$$\left. +\frac{\pi^2}{a_s}\left(\frac{25}{24}\right)k_G\langle\alpha_s G^2\rangle^2\tau^4\right\}, \quad (26)$$

from which one can deduce the ratio $\mathcal{R}^c_{10}(\tau)$. $\gamma_E = 0.5772...$ is the Euler constant and:

$$\rho^c_n = 1 - e^{-t_c\tau}\left(1 + (t_c\tau) + \cdots + \frac{(t_c\tau)^n}{n!}\right). \quad (27)$$

• *Strategies*

◇ *Parametrization of the spectral function*

To a first approximation, we have parametrized the spectral function using the minimal duality ansatz (MDA):

$$\frac{1}{\pi}\mathrm{Im}\,\tilde{\psi}(t) = f_T^2 M_T^4\delta(t - M_T^2) + \theta\left(t\_t_c\right)\ \text{“QCD continuum”}, \quad (28)$$

where we assume that the QCD expression of the spectral function above the continuum threshold t_c smears all radial excitation contributions. f_T is normalized as $f_\pi = 132$ MeV. In the MDA parametrization:

$$\mathcal{R}^c_{10} \simeq M_T^2. \quad (29)$$

◇ *Optimization procedure*

One can notice that there are three free parameters in the analysis, namely the LSR variable τ, the continuum threshold t_c and the perturbative subtraction constant ν. The later quantity is eliminated when one works with different derivatives of the two-point function for taking its inverse Laplace transform and working with the running QCD parameters. The optimal results will be extracted at the minimum or inflexion points in τ while we shall fix the range of t_c in a conservative region from the beginning of τ-stability until the (approximate) t_c-stability.

◇ *QCD input parameters*

We shall work with the QCD input parameters [9,10]:

$$\Lambda = 340(28)\ \text{MeV}, \quad \langle\alpha_s G^2\rangle = (6.49 \pm 0.35)10^{-2}\ \text{GeV}^4, \quad (30)$$

and use the parametrization of the $D = 8$ gluon condensates given in Eq. (7).

• *Di-gluonium mass and coupling at Lowest Order (LO)*

In this section, we redo the analysis in Ref. [4] using the expression in Eq. (5) that one shall explicitly compare with the one including the new NLO terms.

◇ We show the determination of M_T from $\mathcal{R}^c_{10}$ in Fig. 4, where the vacuum saturation estimate of the $D = 8$ gluon condensates is assumed. We show the t_c-behaviour of the optimal values on τ in Fig. 5. The final optimal results are obtained for the set (τ, t_c) from (0.18,4.5) to (0.68,12) (GeV^{-2}, GeV^2) and are respectively 1857 and 2324 MeV. They lead to the mean:

$$M_T = 2091(234)_{t_c}(24)_{G^2}\ \text{MeV} \ \multimap\!\!\!\rightarrow\ t_c \simeq \left(6.5^{+5.5}_{-2.0}\right)\ \text{GeV}^2. \quad (31)$$

◇ We show the analysis of the coupling f_T from the moment $\mathcal{L}^c_0$ in Fig. 6.

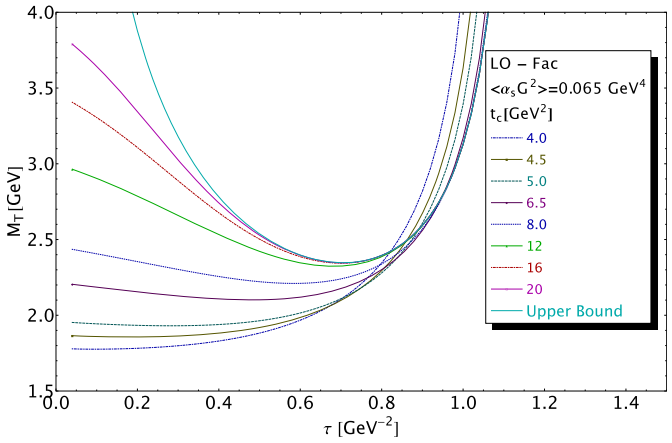

Fig. 4. Behaviour of the 2^{++} tensor di-gluonium mass from the ratio of moments $\mathcal{R}_{10}^{c}$ versus τ for different values of t_c at LO.

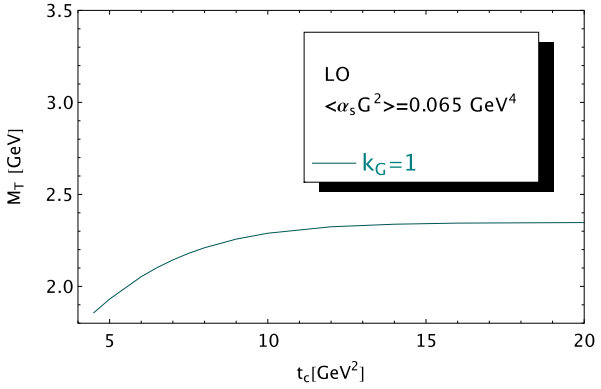

Fig. 5. t_c-behaviour of the 2^{++} tensor di-gluonium LO mass at the τ minimum.

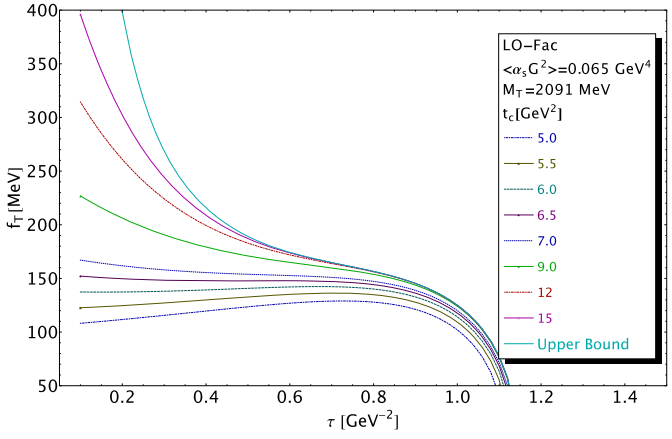

Fig. 6. Behaviour of the 2^{++} tensor di-gluonium coupling from the moment $\mathcal{L}_0^c$ versus τ for different values of t_c at LO assuming a factorization of the $D=8$ condensates ($k_G=1$).

– One obtains:

$$f_T = 156(9)_{t_c}(0.4)_{G^2}(22)_{M_T}\ \text{MeV} \ \leftrightarrow\!\!\!\rightarrow\ t_c \simeq \left(7.0^{+5.0}_{-0.5}\right)\ \text{GeV}^2. \tag{32}$$

These results agree within the errors with the ones in Eq. (1) obtained at slightly low value of $t_c \simeq 5.5$ GeV^2. The large error obtained here is due to the most conservative choice of the t_c-range.

– We obtain the central values of the upper bounds:

$$M_T \leq 2347\ \text{MeV}, \qquad f_T \leq 174\ \text{MeV}. \tag{33}$$

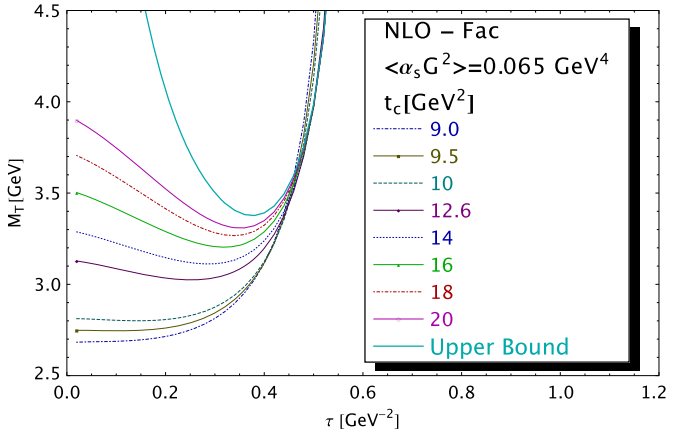

Fig. 7. Behaviour of the 2^{++} tensor di-gluonium mass from the ratio of moments $\mathcal{R}_{10}^{c}$ versus τ for different values of t_c at NLO assuming a factorization of the $D=8$ condensates ($k_G=1$).

The bound on the mass is comparable with the one in Eq. (1).

- *The 2^{++} ground state di-gluonium mass at NLO*
  - ◇ *Factorization of the $D=8$ gluon condensates ($k_G=1$)*

The behaviour of the mass is shown in Fig. 7 where we have assumed the factorization of the dimension 8 gluon condensates. The stabilities in τ are reached for the set $(\tau, t_c) = (0.12, 9.5)$ to (0.36,20) (GeV^{-2}, GeV^2) to which correspond the mass values 2746 and 3309 MeV.

– We deduce the mean value:

$$\begin{aligned}\langle M_T\rangle &= 3028(281)_{t_c}(1)_{\tau}(34)_{\Lambda}(47)_{G^2}\\ &\quad (243)_{PT}(207)_{PT_{G^2}}(0)_{OPE}\ \text{MeV}\\ &= 3028(429)\ \text{MeV} \ \leftrightarrow\!\!\!\rightarrow\ t_c \simeq \left(12.6^{+7.4}_{-3.1}\right)\ \text{GeV}^2.\end{aligned} \tag{34}$$

We have added some systematic errors: the last 5th and 6th errors come from an estimate of the higher order (HO) α_s corrections to the PT and $\langle\alpha_s G^2\rangle$ contributions where the α_s^n coefficients are assumed to increase geometrically [23]. The last 7th error comes from the high-dimension condensates estimated to be about $(\Lambda^2\tau)$ times the $\langle G^4\rangle$ contributions.

– From Fig. 7, one can also deduce the optimal upper bound from the positivity of the ratio of moments. We obtain:

$$\begin{aligned}M_T &\leq 3376(26)_{\Lambda}(42)_{G^2}(240)_{PT}(286)_{PT_{G^2}}\\ &\leq 3376(377)\ \text{MeV}.\end{aligned} \tag{35}$$

- ◇ *Comparison with the LO results within factorization*

We notice that the PT NLO corrections increase the central value of the mass by 561 MeV from its LO value while the $\langle\alpha_s G^2\rangle$ ones provide an additional increase of 376 MeV.

- ◇ *Comparison with some other LSR results*

– In Ref. [24], the result:

$$M_T = 1.86^{+014}_{-0.17}\ \text{GeV} \tag{36}$$

has been obtained to LO PT but including the NLO $\langle\alpha_s G^2\rangle$ term and the LO constant term of the $\langle gG^3\rangle$ condensates. Unfortunately, our results summarized in Eq. (23) do not agree with the coefficients of these condensates. The difference of these coefficients may come from the different current used by Ref. [24].

– Result within instanton liquid model is about 1525 MeV [25] which is much lower than our above result.

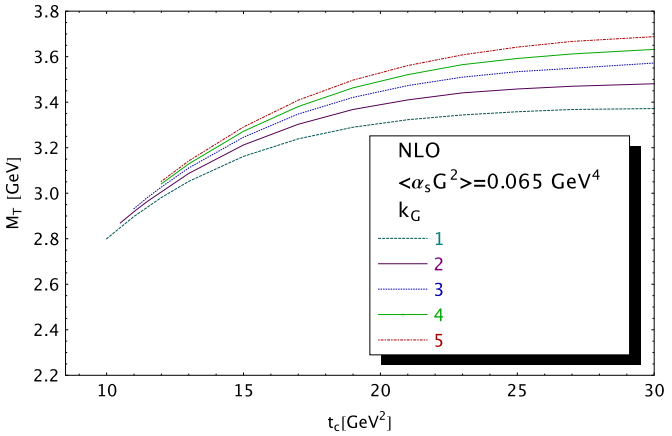

Fig. 8. Behaviour of the 2^{++} tensor di-gluonium mass versus t_c for different values of the factorization factor k_G.

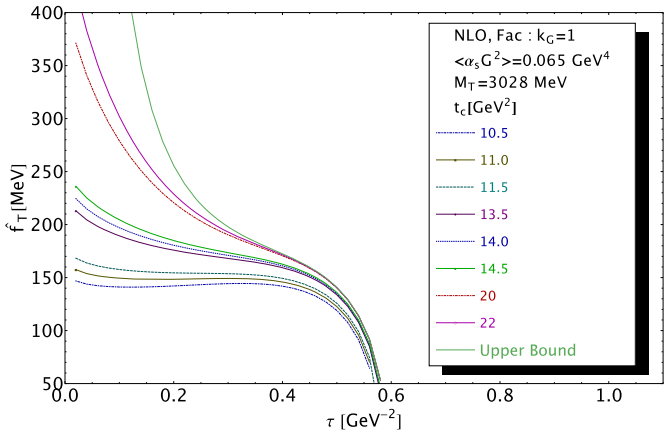

Fig. 9. Behaviour of the 2^{++} tensor di-gluonium RGI coupling from the moment $\mathcal{L}_0^c$ versus τ for different values of t_c at NLO within factorization.

◇ *Effect of the $D=8$ condensates*

Now, we study the effect of the estimate of the $D=8$ gluon condensates on the mass determination assuming that the factorization can be violated like in the case of the four-quark condensate. The analysis is similar to the one in Fig. 7. We show the optimal results in Fig. 8 versus t_c for different values of the violation factor k_G.

One can notice that the value of the mass is a smooth increasing function of k_G. From the vacuum saturation estimate ($k_G=1$) to 5 (if one takes the same value as the violation of the four-quark condensate), the value of the mass moves from 3028(287) MeV to 3347(295) MeV thus an increase of about 319 MeV.

◇ *Final estimate of the mass at NLO*

For definiteness, we shall work with the conservative range:

$$k_G = (3 \pm 2). \tag{37}$$

– Then, we deduce the final estimate:

$$\begin{aligned}\langle M_T\rangle &= 3188(291)_{t_c}(34)_\Lambda(47)_{G^2}(159)_{k_G}\\ &\quad (157)_{PT}(162)_{PT_{G^2}}(2)_{OPE}\ \text{MeV}\\ &= 3188(405)\text{MeV},\end{aligned} \tag{38}$$

which corresponds to $t_c \approx \left(14.1^{+7.9}_{-3.1}\right)$ GeV^2.

– The related absolute upper bound is:

$$\begin{aligned}M_T &\leq 3580(17)_\Lambda(45)_{G^2}(168)_{k_G}\\ &\quad (210)_{PT}(198)_{PT_{G^2}}(8)_{OPE}\ \text{MeV}\\ &\leq 3580(338)\ \text{MeV}.\end{aligned} \tag{39}$$

Our result for the ground state mass is in line with the ones from some other approaches [26] and ADS/QCD [27] where its mass is expected to be above 2 GeV. It is slightly higher than recent lattice calculations in the range (2.27 ∼ 2.67) GeV [28–30].

• *The 2^{++} ground state di-gluonium coupling at NLO*

We introduce the renormalization group invariant (RGI) coupling $\hat{f}_T$ which is related to the running coupling $f_T(\nu)$ associated to the two-point correlator $\tilde{\psi}_T$ as:

$$f_T(\nu) = \frac{\hat{f}_T}{\left(\log\frac{\nu}{\Lambda}\right)^{\frac{\gamma_1}{-2\beta_1}}} \qquad : \qquad \gamma_1 = \frac{n_f}{3}. \tag{40}$$

We shall extract the coupling from the lowest moment $\mathcal{L}_0^c$.

◇ *Factorization of the $D=8$ gluon condensates ($k_G=1$)*

– The NLO analysis is shown in Fig. 9. One can notice that, in the presence of the NLO terms (PT and $\langle\alpha_s G^2\rangle$), the curves present more pronounced minimum and inflexion points. The curves present a minimum at 148 MeV and inflexion point at 193 MeV for the set (τ, t_c) equals to (0.2,11) and (0.3,22) (GeV^{-2}, GeV^2). One obtains to NLO:

$$\begin{aligned}\hat{f}_T|_{NLO} &= 167(25)_{t_c}(1)_\tau(1.5)_\Lambda(1)_{G^2}(25)_{M_T}\\ &\quad (16)_{PT}(11)_{PT_{G^2}}(0)_{OPE}\ \text{MeV}\\ &= 167(40)\ \text{MeV} \ \leftrightarrow\!\!\circ\!\!\rightarrow\ t_c \simeq \left(14^{+8}_{-3}\right)\ \text{GeV}^2,\end{aligned} \tag{41}$$

and the optimal upper bound at the inflexion point $\tau \simeq 0.3$ GeV^{-2}:

$$\begin{aligned}\hat{f}_T|_{NLO} &\leq 186(1)_\Lambda(2)_{G^2}(32)_{M_T}(2)_{PT}(11)_{PT_{G^2}}(0)_{OPE}\ \text{MeV}\\ &\leq 186(34)\ \text{MeV},\end{aligned} \tag{42}$$

where we have used the mass value in Eq. (34).

– Comparing with the LO result, one can notice that the change of the mass from 2091 to 3028 MeV has slightly increased the coupling by about 58 MeV while fixing the mass at its LO value, the NLO corrections have only increased the coupling by 13 MeV.

◇ *Beyond the factorization of the $D=8$ gluon condensates*

We extract the value of the coupling corresponding to the k_G-factor in Eq. (37). The curves are shown in Fig. 10. One obtains for the set of (τ, t_c): (0.12, 12) and (0.30, 22) in (GeV^{-2}, GeV^2) the values 156.6 and 173.6 MeV which give:

$$\begin{aligned}\hat{f}_T &= 164(8)_{t_c}(3)_\Lambda(1.3)_{G^2}(3)_{k_G}(20)_{M_T}\\ &\quad (16)_{PT}(5)_{PT_{G^2}}(0)_{OPE}\ \text{MeV}\\ &= 164(28)\ \text{MeV}, \ \leftrightarrow\!\!\circ\!\!\rightarrow\ t_c \simeq \left(12.5^{+9.5}_{-0.5}\right)\ \text{GeV}^2,\end{aligned} \tag{43}$$

and the optimal upper bound at the inflexion point $\tau \simeq 0.3$ GeV^{-2}:

$$\begin{aligned}\hat{f}_T|_{NLO} &\leq 203(5)_\Lambda(2)_{G^2}(5)_{k_G}(28)_{M_T}\\ &\quad (19)_{PT}(11)_{PT_{G^2}}(0)_{OPE}\ \text{MeV}\\ &\leq 203(36)\ \text{MeV}.\end{aligned} \tag{44}$$

We notice that, like the mass, the value of the coupling is weakly affected by the value of the $D=8$ gluon condensates.

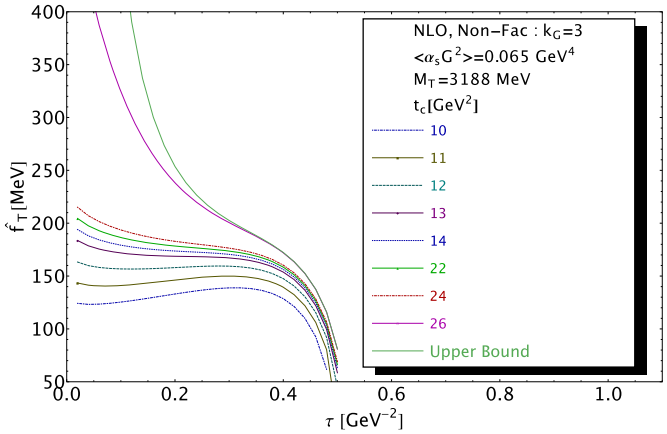

Fig. 10. Behaviour of the 2^{++} tensor di-gluonium RGI coupling from the moment $\mathcal{L}_0^c$ versus τ for different values of t_c at NLO without factorization.

7. Summary and conclusions

⋄ We have computed the perturbative and $\langle\alpha_s G^2\rangle$ NLO corrections to the 2^{++} tensor di-gluonium two-point correlator and use the method of Laplace transform sum rules (LSR) to revise the estimate of the mass and coupling of the lowest ground state.

⋄ We find that the LO $\langle\alpha_s G^2\rangle$ coefficient has no imaginary part like found by NSVZ [1] but the constant term is not zero in contrast to NSVZ who have used dual/anti-dual field arguments. Thus, the use of the RGE allows to fix its $\log(Q^2/\nu^2)$ NLO coefficient from this LO constant term.

⋄ We note that our LO coefficient of $\langle g\,G^3\rangle$ disagrees with the one of [24] but agrees with the one of NSVZ. This disagreement may be related to the choice of current. As an indirect check of our result, we recalculate the $\langle g\,G^3\rangle$ coefficient in the scalar gluonium channel and recover the one of NSVZ.

⋄ Assuming vacuum saturation for the estimate of the $D=8$ gluon condensates, we found the lowest ground state mass $M_T = 3028(429)$ MeV (Eq. (34)) and RGI coupling $\hat{f}_T = 167(40)$ MeV (Eq. (41)). We also obtain the absolute upper bounds related to the positivity of the spectral function: $M_T \leq 3376(377)$ MeV (Eq. (35)) and $\hat{f}_T \leq 186(34)$ MeV (Eq. (42)).

⋄ We study the effect of the estimate of the $D=8$ gluon condensates. We find $M_T = 3188(405)$ MeV (Eq. (38)) and $\hat{f}_T = 164(28)$ MeV (Eq. (43)) for the violation factor $k_G = (3 \pm 2)$. We also deduce the upper bounds: $M_T \leq 3580(338)$ MeV (Eq, (39)) and $\hat{f}_T \leq 203(36)$ MeV (Eq. (44)).

⋄ Our result is in line with the ones from some other approaches [26] and ADS/QCD [27] where its mass is expected to be above 2 GeV. However, the central value of our mass is slightly higher than lattice calculations in the range $(2.27 \sim 2.67)$ GeV [28–30].

⋄ Our result does not favour the interpretation of the observed $f_2(2010, 2300, 2340)$ states as pure gluonia/glueball candidates (see e.g. [31]). Moreover, we do not expect that an eventual meson-gluonium mixing will affect our result as this mixing is expected to be small $(\theta \simeq -10^0)$ [14].

Acknowledgement

TGS is grateful for research funding from the Natural Sciences and Engineering Research Council of Canada (NSERC).

Declaration of competing interest

The authors declare that they have no known competing financial interests or personal relationships that could have appeared to influence the work reported in this paper.

Data availability

No data was used for the research described in the article.

References

[1] V.A. Novikov, M.A. Shifman, A.I. Vainshtein, V.I. Zakharov, Nucl. Phys. B 191 (1981) 301.
[2] S. Narison, Z. Phys. C 22 (1984) 161.
[3] S. Narison, QCD spectral sum rules, World Sci. Lect. Notes Phys. 26 (1989) 1–527.
[4] S. Narison, Nucl. Phys. B 509 (1998) 312;
S. Narison, Nucl. Phys. B, Proc. Suppl. 64 (1998) 210.
[5] R.L. Workman, et al., Particle Data Group, PTEP 2022 (2022) 083C01.
[6] M.A. Shifman, A.I. Vainshtein, V.I. Zakharov, Nucl. Phys. B 147 (1979) 385, 448.
[7] K.G. Chetyrkin, S. Narison, V.I. Zakharov, Nucl. Phys. B 550 (1999) 353.
[8] For a review, see e.g.: S. Narison, QCD as a theory of hadrons, Camb. Monogr. Part. Phys. Nucl. Phys. Cosmol. 17 (2004) 1–778, arXiv:hep-ph/0205006.
[9] S. Narison, Nucl. Part. Phys. Proc. 324 (329) (2023) 94, and references therein.
[10] S. Narison, Nucl. Phys. A 1039 (2023) 122744.
[11] T. de Oliveira, D. Harnett, A. Palameta, T.G. Steele, Phys. Rev. D 106 (2022) 114023.
[12] J.C. Collins, An Introduction to Renormalization, the Renormalization Group, and the Operator Product Expansion, Cambridge University Press, 1986.
[13] S. Narison, Phys. Rep. 84 (4) (1982) 263.
[14] E. Bagan, A. Bramon, S. Narison, Phys. Lett. B 196 (1987) 203.
[15] N. Pak, S. Narison, N. Paver, Phys. Lett. B 147 (1984) 162.
[16] A.A. Pivovarov, Phys. At. Nucl. 63 (2000) 1646;
A.A. Pivovarov, Yad. Fiz. 63 (9) (2000) 1734.
[17] V.A. Novikov, M.A. Shifman, A.I. Vainshtein, V.I. Zakharov, Nucl. Phys. B 174 (1980) 378.
[18] D. Asner, R.B. Mann, J.L. Murison, T.G. Steele, Phys. Lett. B 296 (1992) 171.
[19] S. Narison, E. de Rafael, Phys. Lett. B 522 (2001) 266.
[20] S. Narison, The Laplace transform and its applications, arXiv:2309.00258[hep-ph], to appear in Nova Science Pub., New-York, ed. V. Matinez-Luaces.
[21] J.S. Bell, R.A. Bertlmann, Nucl. Phys. B 177 (1981) 218;
J.S. Bell, R.A. Bertlmann, Nucl. Phys. B 187 (1981) 285.
[22] R.A. Bertlmann, Acta Phys. Austriaca 53 (1981) 305.
[23] S. Narison, V.I. Zakharov, Phys. Lett. B 522 (2001) 266.
[24] H.-X. Chen, W. Chen, S.-L. Zhu, Nucl. Part. Phys. Proc. 318 (323) (2022) 122, Phys. Rev. D 104 (9) (2021) 094050.
[25] J. Chen, J. Liu, Phys. Rev. D 95 (2017) 014024.
[26] For a review, see e.g.: V. Mathieu, N. Kochelev, V. Vento, Int. J. Mod. Phys. E 18 (2009) 1.
[27] L. Zhang, C. Chen, Y. Chen, M. Huang, Phys. Rev. D 105 (2022) 026020.
[28] Y. Chen, et al., Phys. Rev. D 73 (2006) 014516.
[29] E. Gregory, et al., J. High Energy Phys. 1210 (2012) 170, and references therein.
[30] A. Athenodorou, M. Teper, J. High Energy Phys. 11 (2020) 172.
[31] E. Klempt, A.V. Sarantsev, I. Denisenko, K.V. Nikonov, Phys. Lett. B 830 (2022) 137171.